Anonymous Referee #1

This manuscript reports the measurement of 13 SOA tracers from both biogenic and anthropogenic precursors in the particulate samples collected at Nam Co. The seasonal variations of isoprene SOA, monoterpene SOA and aromatic SOA tracers at Nam Co were interpreted by the temperature effect on the precursor emission and gas/particle partitioning. Source apportionment was carried by using the SOA-tracer method and the backward trajectory analysis. This is a well written paper and could be accepted by ACP if the following issues were addressed.

1. The temperature change could have two opposite effects on the SOA production. Decreasing temperature could reduce the precursor emission but enhance the gas to particle partitioning. The interpretations of the seasonal variation of SOA levels are quite confusing. It would be much better to develop a simple model to quantitatively or semi-quantitatively evaluate the temperature effect here and reveal which process (emission or partitioning) is dominant.

Reply: We appreciate the suggestion. In the revised manuscript, we used the two-product model to estimate the temperature effect on partitioning. SOA yield (Y) of precursors could be expressed using an empirical relationship based on gas-particle partitioning of two semi-volatile products (Odum et al., 1996):

$$Y = M_0 \sum_{i}^{2} \frac{\alpha_i K_i}{1 + M_0 K_i}$$

where M_0 (μg m^{-3}) is the total concentration of absorbing organic material; α_i is the mass stoichiometric coefficient of the product *i*; K_i (m^3 μg^{-1}) is the temperature-dependent partitioning coefficient of the semi-volatile compound *i*. Assuming a constant activity coefficient and mean molecular weight, partitioning coefficient, K_i (T) at a certain temperature (T) could be estimated (Sheehan and Bowman, 2001):

$$K_i(T) = K_i^* \frac{T}{T^*} \, exp\left[\frac{H_i}{R}\left(\frac{1}{T} - \frac{1}{T^*}\right)\right]$$

Where K_i^* is an experimentally determined partitioning coefficient at a reference temperature, T^*; H_i is the vaporization enthalpy; R is the gas constant. To model the temperature-dependent absorptive partitioning, three parameters, α_i, K_i, and H_i, are required for each condensable product.

Table 1 lists all the parameters for the two-product model of α-pinene SOA which were also used to estimate the temperature effect on SOA partitioning by Sheehan and Bowman (2001). The available data of OC at the NC site were reported in the range of 1.18 to 2.26 μgC m^{-3} during July 2006 to January 2007 with an average of 1.66 μgC m^{-3} (Ming et al., 2010). Thus, M_0 is calculated as 2.32 μg m^{-3} by the average OC multiplying 1.4.

Table 1 Two-product model parameters for α-pinene SOA

α_1	0.038
α_2	0.326
K_1^* (mg/μg)	0.171

K_2^* (mg/μg)	0.004
T* (K)	308
H_1=H_2 (kcal/mol)	17.5
R (J/K mol)	8.314

Monoterpene emission rate is solely dependent on temperature. The activity factor (γ_T) is expressed as (Guenther et al., 1993):

$$\gamma_T = exp^{\beta(T-T_s)}$$

Figure 1 shows the temperature dependence of α-pinene emission rate (γ_T) and SOA yield within the temperature range at the NC site. Obviously, decreasing temperature could reduce the precursor emission but enhance the gas to particle partitioning and SOA yield.

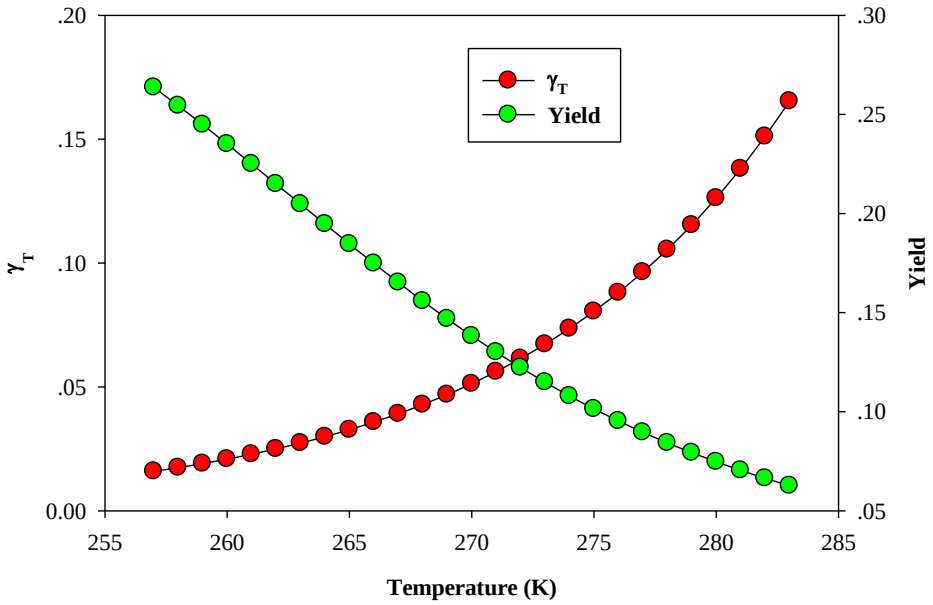

Figure 1 Temperature dependence of α-pinene emission rate (γ_T) and SOA yield

From July to November 2012 (period 1), high values of SOA_M tracers and SOA yield existed under low temperature, and SOA_M tracers were positively correlated with SOA yield (r=0.647, p<0.05, Figure 2a). These suggested that the temperature effect on partitioning was the dominant process influencing SOA variation during period 1. From December 2012 to April 2013 (period 2), high values of SOA_M tracers and activity factor (γ_T) existed under high temperature, and SOA_M tracers were positively correlated with γ_T (r=0.741, p<0.05, Figure 2b). These suggested that the temperature effect on emission was the dominant process influencing SOA variation during period 2. From May to July 2013 (period 3), SOA_M tracer concentrations were relative stable, and there was no correlation of SOA_M tracers with γ_T or SOA yield (p>0.05). These might result from the counteraction of temperature effects on emission and partitioning during the period 3.

These interpretations of the seasonal variation of monoterpene SOA tracers were added in the revised manuscript (See below). Figure 2 was added in the revised

manuscript as Figure 5. Figure 1 and Table 1 were added in the supplemental information file as Figure S5 and Table S2, respectively.

"SOA yield (Y) of precursors could be expressed using an empirical relationship based on gas-particle partitioning of two semi-volatile products (Odum et al., 1996):

$$Y = M_0 \sum_i^2 \frac{\alpha_i K_i}{1+M_0 K_i} \quad (8)$$

where M_0 (μg m^{-3}) is the total concentration of absorbing organic material, α_i is the mass stoichiometric coefficients of the product i, K_i (m^3 μg^{-1}) is the temperature-dependent partitioning coefficient of the semi-volatile compound i. Assuming a constant activity coefficient and mean molecular weight, the partitioning coefficient, K_i (T) at a certain temperature (T) could be estimated as (Sheehan and Bowman, 2001):

$$K_i(T) = K_i^* \frac{T}{T^*} exp\left[\frac{H_i}{R}\left(\frac{1}{T} - \frac{1}{T^*}\right)\right] \quad (9)$$

where K_i^* is an experimentally determined partitioning coefficient at a reference temperature, T^*. H_i is the vaporization enthalpy, R is the gas constant. To model the temperature-dependent absorptive partitioning, three parameters, α_i, K_i, and H_i, are required for each condensable product.

Table S2 lists all the parameters for two-product model of α-pinene SOA which were also used to estimate the temperature effect on SOA partitioning by Sheehan and Bowman (2001). The available data of OC at the NC site were reported in the range of 1.18 to 2.26 μgC m^{-3} during July 2006 to January 2007 with an average of 1.66 μgC m^{-3} (Ming et al., 2010). Thus, M_0 is calculated as 2.32 μg m^{-3} by the average OC multiplying 1.4. Figure S5 shows the temperature dependence of α-pinene emission rate (γ_T) and SOA yield within the temperature range at the NC site (-16.7 to 10.2 ℃). Obviously, decreasing temperature could reduce the emission but enhance the gas to particle partitioning and SOA yield.

From July to November 2012 (period 1), high values of SOA_M tracers and SOA yield existed under low temperature, and SOA_M tracers were positively correlated with SOA yield ($r=0.647$, $p<0.05$, Figure 5a). These suggested that the temperature effect on partitioning was the dominant process influencing SOA_M tracers' variation during the period 1. From December 2012 to April 2013 (period 2), high values of SOA_M tracers and activity factor (γ_T) existed under high temperature, and SOA_M tracers were positively correlated with γ_T ($r=0.741$, $p<0.05$, Figure 2b). These suggested that the temperature effect on emission was the dominant process influencing SOA_M tracers' variation during the period 2. The increase of SOA_M tracer concentrations during spring was also observed in the southeastern United States (Ding *et al.* 2008), resulting from the enhancement of monoterpenes emission in spring (Kim et al., 2011). From May to July 2013 (period 3), SOA_M tracer concentrations were relative stable, and there was no correlation of SOA_M tracers with γ_T or SOA yield ($p>0.05$). These might result from the counteraction of temperature effects on emission and partitioning during the summer."

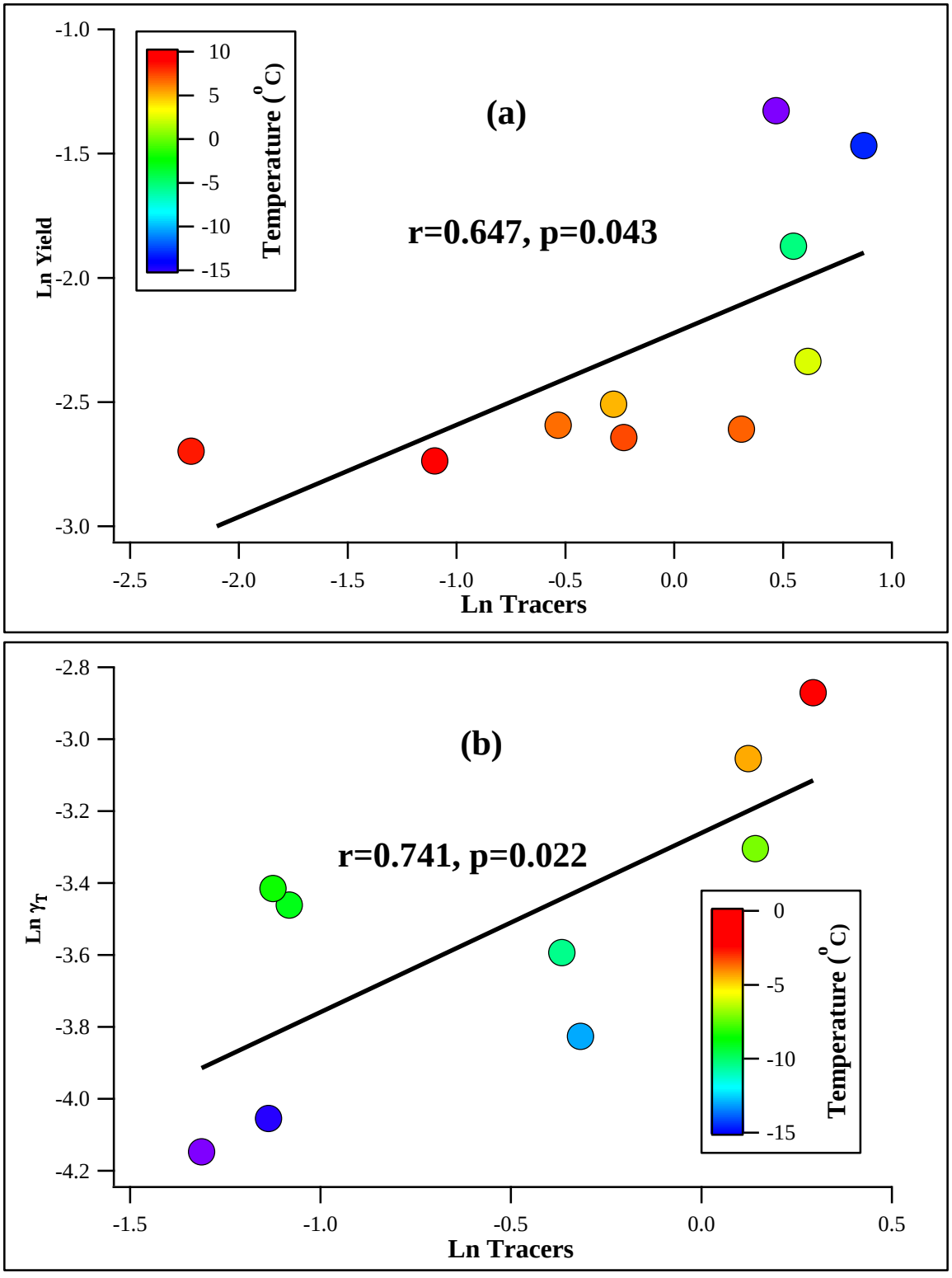

Figure 2 Correlation of monoterpene SOA tracers (SOA_M tracers) with SOA yield in period 1 (a) and γ_T in period 2 (b).

For isoprene, the reactive uptake of epoxides onto particles plays the key role (Lin et al., 2013; Paulot et al., 2009) in isoprene SOA formation. Obviously, high temperature could enhance heterogeneous reactions and result in high levels of isoprene

SOA. Figure 3a presents a negative correlation between the natural logarithm of SOA_I tracer levels and the reciprocal of temperature in Kelvin ($p<0.001$). Moreover, the temperature dependence of SOA_I tracers was similar to that of C_T, and SOA_I tracers exhibited a significant positive correlation with C_T during our sampling at the NC site (Figure 3b). These results indicated that the seasonal variation of SOA_I tracers at the NC site was mainly influenced by isoprene emission.

These discussions about the seasonal variation of isoprene SOA tracers were added in the revised manuscript as "Figure 3a presents a negative correlation between the natural logarithm of SOA_I tracer levels and the reciprocal of temperature in Kelvin ($p<0.001$). Moreover, the temperature dependence of SOA_I tracers was similar to that of C_T, and SOA_I tracers exhibited a significant positive correlation with C_T during our sampling at the NC site (Figure 3b). These results indicated that the seasonal variation of SOA_I tracers at the NC site was mainly influenced by isoprene emission. Considering the short lifetime (several hours) of isoprene in the air, SOA_I should be mainly formed from local precursor. In summer, high temperature and intense light could enhance isoprene emission and photo-reactions. Moreover, high temperature in summer could enhance the heterogeneous reactions of isoprene-derived epoxides on particles which play key roles in isoprene SOA formation (Lin et al., 2013; Paulot et al., 2009). All these interpreted the high levels of isoprene SOA tracers in the summer at the NC site."

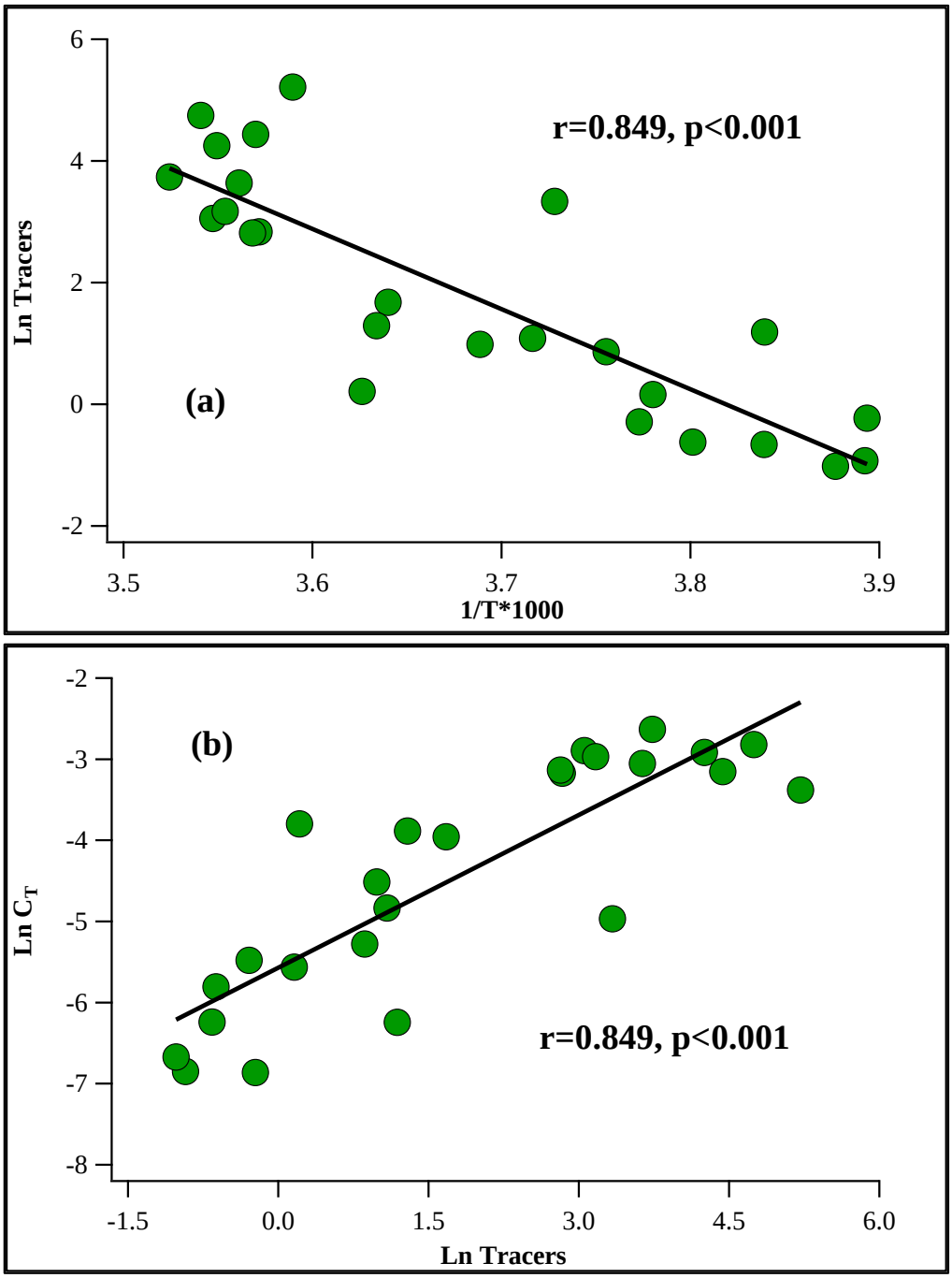

Figure 3 Correlations of SOA_I tracers with temperature (a) and C_T (b)

2. The large uncertainty of the SOA-tracer method and the simple backward trajectory analysis make the source apportionment in this work not very convincible. More detailed information about the anthropogenic emissions from Indian subcontinent and inland China would be helpful for the SOA source apportionment.

Reply: Yes, we agree. Unfortunately, emission inventories are not available in the Indian subcontinent and the Tibetan Plateau. Instead, we looked up the satellite data of population density (Socioeconomic Data and Applications Center, http://sedac.ciesin.columbia.edu/maps/gallery/search?facets=theme:population), aerosol optical thickness (AOT, NASA Earth Observations,

http://neo.sci.gsfc.nasa.gov/), tropospheric NO_2 vertical column densities (VCD, The Aura Validation Data Center, http://avdc.gsfc.nasa.gov/), and surface CO (https://www2.acd.ucar.edu/mopitt) on the global scale. As shown in Figure 4a, the northern Indian subcontinent (area within the red circle) was the most populated region of the world, with a population density of more than 1000 persons per km^2. Moreover, the plots of global AOT, tropospheric NO_2 VCD, and surface CO (Figure 4, b-d) all illustrated that the northern Indian subcontinent, including Bangladesh, Nepal, the northeastern India, and the northwestern India was the global hotspots of these anthropogenic pollutants. Compared with the northern Indian subcontinent, the Tibetan Plateau exhibited extremely low population density and low levels of AOT, surface CO, and NO_2 VCD (Figure 5, a-d). Besides these satellite data, a recent study at a site in the northwestern India (Indo-Gangetic plain) witnessed extremely high levels (up to 2065 ng m^{-3}) of polycyclic aromatic hydrocarbons which were mainly from anthropogenic combustion processes (Dubey et al., 2015). All these demonstrated that there were high anthropogenic emissions in the northern India subcontinent.

In the revised manuscript, we added the discussions about the anthropogenic emissions in the India subcontinent (see below). Figure 4 and 5 were added in the supplemental information file and the revised manuscript as Figure S7 and Figure 8, respectively.

"To check the potential source areas of anthropogenic emissions, the satellite data of population density (http://sedac.ciesin.columbia.edu/theme/population), aerosol optical thickness (AOT, http://neo.sci.gsfc.nasa.gov/), tropospheric NO_2 vertical column densities (VCD, http://avdc.gsfc.nasa.gov/), and surface CO (https://www2.acd.ucar.edu/mopitt) were analysis on the global scale. As shown in Figure S7a, the northern Indian subcontinent was the most populated region of the world, with a population density of more than 1000 persons per km^2. Moreover, the plots of global AOT, tropospheric NO_2 VCD, and surface CO (Figure S7, b-d) illustrated that the northern Indian subcontinent, including Bangladesh, Nepal, the northeastern India, and the northwestern India was the global hotspots of these anthropogenic pollutants. Compared with the northern Indian subcontinent, the TP exhibited extremely low population density and low levels of AOT, surface CO, and NO_2 VCD (Figure 8, a-d). Besides these satellite data, a recent study at a site in the northwestern India (Indo-Gangetic plain) witnessed extremely high levels (up to 2065 ng m-3) of polycyclic aromatic hydrocarbons which were mainly from anthropogenic combustion processes (Dubey et al., 2015). All these demonstrated that there were high anthropogenic emissions in the northern India subcontinent."

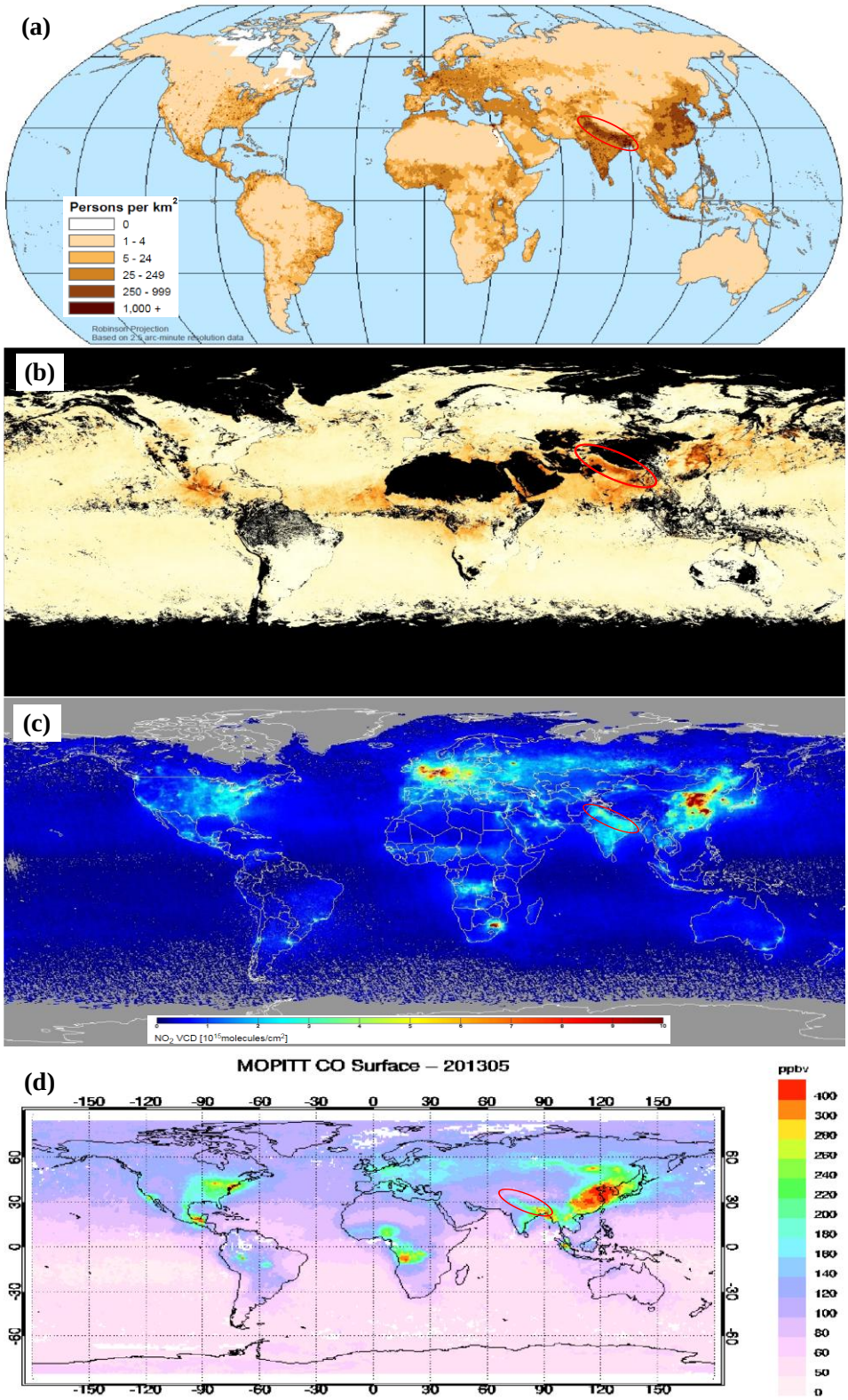

Figure 4 Global distribution of population density in 2000 (a), AOT (b), tropospheric NO_2 VCD (b), and surface CO (d) in May 2013. The area within the red circle is the northern India subcontinent.

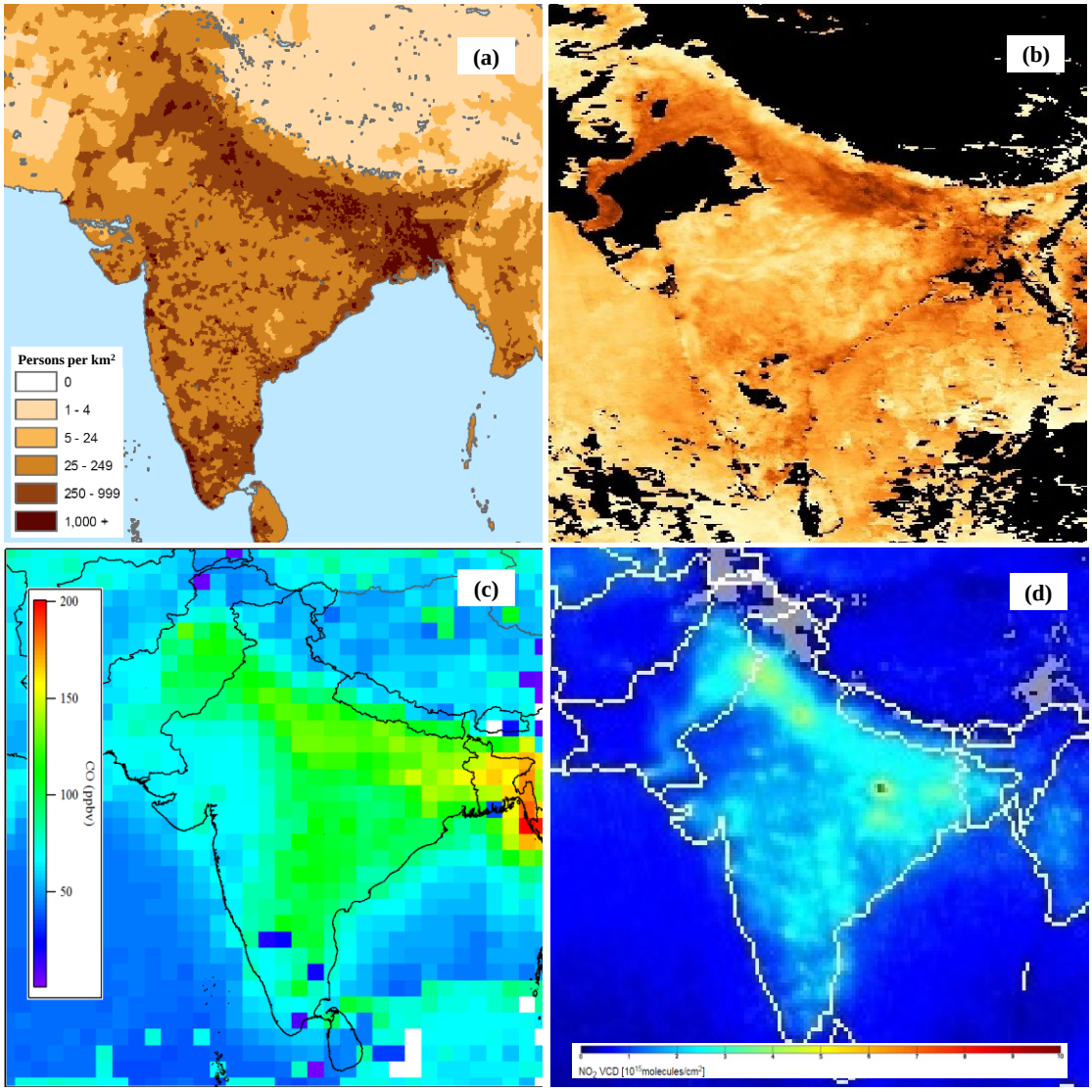

Figure 5 Distribution of population density in 2000 (a), AOT (b), surface CO (c), and NO_2 VCD (d) in May 2013 over the Indian subcontinent and the TP.

References

Dubey, J., Maharaj Kumari, K., and Lakhani, A.: Chemical characteristics and mutagenic activity of $PM_{2.5}$ at a site in the Indo-Gangetic plain, India, Ecotoxicol. Environ. Saf., 114, 75-83, 2015.

Guenther, A. B., Zimmerman, P. R., Harley, P. C., Monson, R. K., and Fall, R.: Isoprene and monoterpene emission rate variability: Model evaluations and sensitivity analyses, J. Geophys. Res.-Atmos., 98, 12609-12617, 1993.

Lin, Y.-H., Zhang, H., Pye, H. O. T., Zhang, Z., Marth, W. J., Park, S., Arashiro, M., Cui, T., Budisulistiorini, S. H., Sexton, K. G., Vizuete, W., Xie, Y., Luecken, D. J., Piletic, I. R., Edney, E. O., Bartolotti, L. J., Gold, A., and Surratt, J. D.: Epoxide as a precursor to secondary organic aerosol formation from isoprene photooxidation in the presence of nitrogen oxides, Proc. Natl. Acad. Sci. U. S. A., 110, 6718-6723, 2013.

Ming, J., Xiao, C., Sun, J., Kang, S., and Bonasoni, P.: Carbonaceous particles in the atmosphere and precipitation of the Nam Co region, central Tibet, J. Environ. Sci., 22, 1748-1756, 2010.

Odum, J. R., Hoffmann, T., Bowman, F., Collins, D., Flagan, R. C., and Seinfeld, J. H.: Gas/particle partitioning and secondary organic aerosol yields, Environ. Sci. Technol., 30, 2580-2585, 1996.

Paulot, F., Crounse, J. D., Kjaergaard, H. G., Kürten, A., St. Clair, J. M., Seinfeld, J. H., and Wennberg, P. O.: Unexpected epoxide formation in the gas-phase photooxidation of isoprene, Science, 325, 730-733, 2009.

Sheehan, P. E., and Bowman, F. M.: Estimated effects of temperature on secondary organic aerosol concentrations, Environ. Sci. Technol., 35, 2129-2135, 2001.